Geochemical modelling of natural geo-/hydrochemical stratification dominated by pyrite oxidation and calcite dissolution in a glaciofluvial Quaternary deposit, Gardermoen, Norway

LEIF BASBERG, ATLE DAGESTAD & PETER ENGESGAARD

Basberg, L., Dagestad, A. & Engesgaard,P. 1998: Geochemical modelling of natural geo-/hydrochemical stratification dominated by pyrite oxidation and calcite dissolution in a glaciofluvial Quaternary deposit, Gardermoen, Norway. *Norges geologiske undersøkelse Bulletin 434*, 35-44.

The PHREEQC geochemical model has been used to reproduce on a geological time scale an abrupt shift between an oxic and an anoxic zone, in the Gardermoen glaciofluvial delta deposit. Groundwater in the aquifer has a major shift in chemical signature three metres below the groundwater table indicating that calcite dissolution and pyrite oxidation are the dominating weathering processes. The results of the modelling have been compared with those of water samples collected from multi-level samplers with microscreens located one metre apart from the groundwater table and five metres down. The sampling scheme was not detailed enough to resolve the exact location of the weathering horizons. The model suggests that the calcite dissolution front is located slightly below the pyrite oxidation front. This causes a significant drop in predicted pH in a zone where other buffering mechanisms than calcite dissolution may become active. Calcite and pyrite in the sediments are of such concentrations that their respective dissolution fronts move at approximately equal rates in the aquifer. The depletion of these minerals has caused a distinct chemical separation in the aquifer between an oxic/low ionic strength and anoxic/high ionic strength zone, that will determine the fate of a contaminant entering the saturated zone.

Leif Basberg & Atle Dagestad, Faculty of Applied Earth Sciences, Division of Geology and Mineral Resources Engineering, Norwegian University of Science and Technology (NTNU), Trondheim, Norway.
Peter Engesgaard, Department of Hydrodynamics and Water Resources, Bldg. 115, Technical University of Denmark, DK-2800 Lyngby, Denmark

Introduction

The capabilities of a geochemical model have been explored with the aim to use the results in a coupled geochemical flow and solute transport model for the Gardermoen aquifer in Norway. Before future scenarios with regard to the hydrochemical development of groundwater affected by natural and anthropogenic events can be hypothesized, it is necessary to understand the existing natural geo-/hydrochemical environment. One-dimensional advective flow coupled with a selection of geochemical reactions provides a tool in which the most reactive minerals in the aquifer matrix can be identified, and the proposed simplification can be tested against field data to check the validity of the proposed model. Identification of natural weathering processes is the first step towards modelling the movement of a leachate plume at the Gardermoen aquifer, since the most active minerals in the weathering processes and their weathering products are likely to respond as leachate enters the aquifer, and because the natural weathering processes may have resulted in a horizontal stratification within the aquifer, establishing units with different geochemical properties.

Field studies of mineral weathering processes in the Gardermoen aquifer have been carried out by several researchers (Teveldal et al. 1990, Jørgensen et al. 1991, Dagestad in prep.). While Teveldal et al. (1990) focused on weathering processes in the soil zone at Nordmoen (Fig. 1), Jørgensen et al. (1991) performed a mass balance study for the whole watershed. A detailed field study was performed by Dagestad (in prep.) at Moreppen II (Fig. 1) where water and sediment samples were collected at one metre intervals. Based on observations made by Dagestad (in prep.), a model was constructed to try to reproduce the observed weathering horizons, and the results of this study are reported in this paper.

Postma et al. (1991) modelled the reduction of nitrate by pyrite oxidation in a Danish aquifer. A similar approach has been adopted in this study to model the weathering processes in a sandy sediment unaffected by anthropogenic activities. One of the aims of the study has been to determine if the concentration of pyrite in the aquifer sediments and its oxidation due to infiltrating oxygen control the propagation of the calcite dissolution front. Although the mineralogy of the aquifer sediments is expected to be similar over the whole aquifer, the individual mineral concentrations might show some variation, but no data to quantify this spatial variation are available.

Geology

The study site is located on the Gardermoen glaciofluvial delta, near the new Oslo airport 60 km northeast of Oslo (Fig.

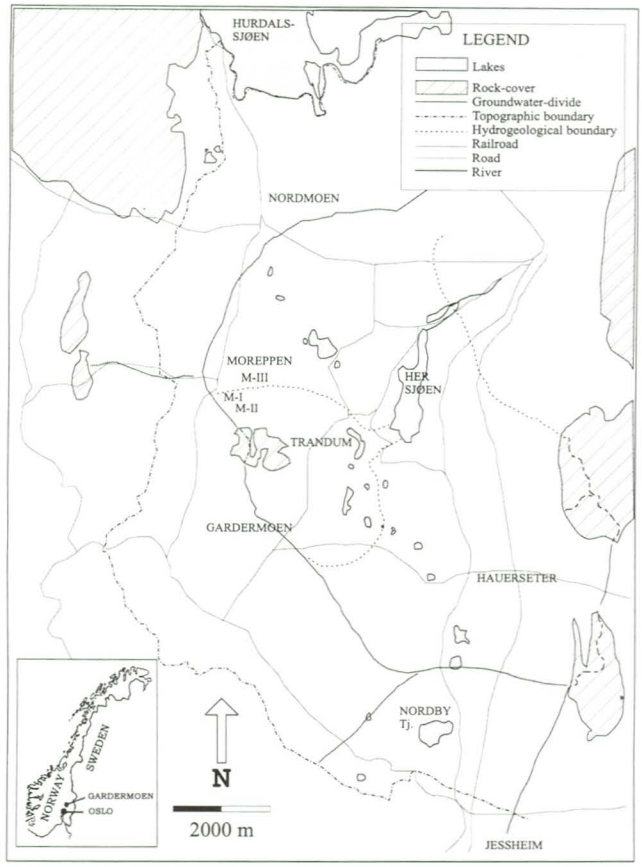

Fig. 1. Study area, Gardermoen.

1). The sediments in the Gardermoen delta were deposited c. 9500 years ago, and geological history of the delta has been described by several authors (e.g. Longva 1987). The hydrostratigraphy of the delta aquifer consists of three main units (Tuttle & Aagaard 1996). The middle hydrostratigraphic unit, corresponding to the delta foreset beds, is the most important unit in terms of groundwater flow since the highly permeable upper (topset) unit is unsaturated. The groundwater drainage pattern is radial (Østmo 1976), with groundwater flowing towards a number of spring ravines discharging at the edge of the delta deposit. The sediments in the area are fairly uniform, and the underlying bedrock consits mainly of gneisses and some granite pegmatites (Longva 1987).

After the final deglaciation, the groundwater table was probably located close to the surface, but due to the subsequent isostatic uplift the groundwater table has been lowered. The shoreline displacement has been estimated to 0.17 m/yr just after the deglaciation, decreasing to 0.12 m/yr 9000 years before the present (Longva 1987). The current rate of isostatic uplift in the area is 0.003 to 0.004 m/year (Andersen & Borns 1994). As the isostatic uplift decreased, the groundwater table became more dependent upon landslides occurring along the edges of the delta and also on recharge. The shift in the controlling mechanism for the location of the groundwater table must have occurred after the most active isostatic uplift ended (Jørgensen et al. 1991). The location of the initial water table is important for the interpretation in this report. If the current groundwater level is at an all time low, then the predicted weathering rates are slightly underestimated; if not, the rates are overestimated (i.e., if the saturated zone has been free to atmospheric oxygen for a considerable time period and over a great depth).

Hydrogeology and geo-/hydrochemistry

The Gardermoen aquifer is a phreatic aquifer that is recharged by infiltrating rain. The initial model setup uses values for mean yearly amounts of infiltration that are distributed evenly throughout the year for the entire simulation period. Henceforth, fluctuations in yearly precipitation, seasonal precipitation and the effects of snow cover, and the subsequent high spring infiltration, have been neglected. A yearly average evapotranspiration of 400 mm has been reported by Jørgensen & Østmo (1990) calculated from pan evaporation measurements during a summer with a yearly precipitation of 800 mm. The same evaporation was also calculated using chloride as a conservative tracer, as suggested by Appelo & Postma (1993), with a net vertical transport of 0.9 m/yr.

Monitoring of groundwater levels has been carried out at two locations at the Gardermoen aquifer over the last thirty years (Kirkhusmo & Sønsterud 1988). These data show that the present location of the groundwater table is low. The depth of the groundwater table varies significantly in the study area, from a few metres at the groundwater divide and up to 30 m in distal areas. Seasonal fluctuations are more significant along the fringes of the groundwater aquifer.

The dissolved concentrations of oxygen and carbon dioxide will be determining factors for the modelled reactions. Recharge water that crosses the water table is saturated with respect to oxygen and the dissolved carbon dioxide pressure has been measured in the field to be approximately ten times the atmospheric pressure, but with seasonal fluctuations (Swendesen et al. 1997, Dagestad in prep.). Unfortunately, the carbon dioxide pressure in the unsaturated zone has not been measured deeper than 2 m below the surface. Nevertheless, measurements made in the lower part of the 2 m-deep unsaturated profile agree well with measurements in the upper part of the saturated zone. As expected, the carbon dioxide pressure stabilizes with depth (Reardon et al., 1979).

Teveldal et al. (1990) performed a detailed study of the silicate weathering rates in a podzol profile with no signs of cultivation at Nordmoen. The highest weathering rates were found near the surface, decreasing to 0.7 m below the surface (m.b.s.), where the silicate composition of the sediments was stabilized and remained constant down to two m.b.s.. The most important weathering processes in the upper soil horizon are the complete breakdown of chlorite and biotite and the transformation of muscovite to vermiculite and smectite.

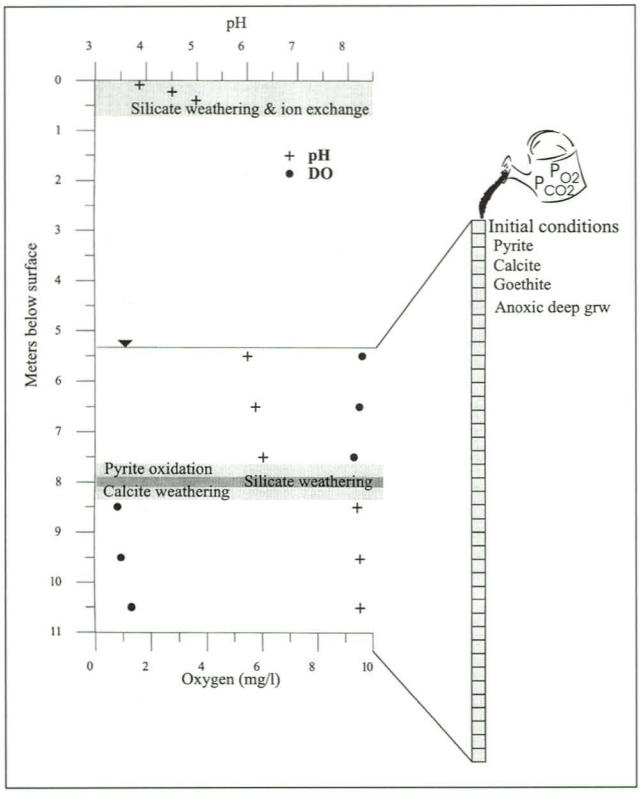

Fig. 2. Model setup and expected horizontal stratification.

A geochemical analysis of the upper 8 m of the soil profile at Moreppen I (Fig. 1) revealed a significant content of iron oxyhydroxides (Skaarstad 1996). This is in accordance with other field studies (Reardon et al. 1979, Postma & Brockenhuss-Schack 1987). Gustafson et al. (1995) also reported on the likely formation of imogolite in sediments in northern Scandinavia. The inclusion of imogolite is necessary in order to perform mass balances of weathering in the upper zone or mass balance studies for the whole watershed.

As the water percolates further down through the unsaturated zone and into the upper saturated zone, only small changes in the water chemistry are noted. When groundwater reaches the pyrite/calcite horizon, it is expected that pyrite oxidation will consume all the available dissolved oxygen and release protons. The lowering of the pH will potentially give rise to silicate weathering, but this is probably confined to a small area just below the pyrite oxidation zone due to the buffering of the acidification by calcite dissolution. The calcite weathering horizon is believed to be located just below the pyrite oxidation zone as shown in Fig. 2.

Groundwater collected from wells located in areas with a different thickness of the unsaturated zone reveals a similar chemical signature; an upper oxic/low ionic strength zone and a lower anoxic/high ionic strength zone. The lower zone has a chemical signature with high calcium and sulphate concentrations that strongly suggests that pyrite oxidation and calcite dissolution are the most important weathering processes (Table 1). The strongest indication of this is found at Moreppen II (Dagestad in prep.) where both sediment samples (Fig. 3), and water samples (Fig. 7) from the same profile have been collected at regular intervals. The data do not resolve the location of the pyrite and calcite weathering horizons relative to each other, only that they are located between 7.5 and 8.5 m.b.s. (~3 m below the water table). A study by Rudolph-Lund (1997) at Moreppen III (Fig. 1) using multi-level samplers located from 4-7 m.b.s. shows no signs of pyrite or calcite weathering. Except for studies at Moreppen II and III samples are collected from wells with filter screens varying in length between one and six metres. The interpretation with respect to horizontal stratification may therefore be seriously distorted due to sample averaging over the length of the filter (Martin-Hayden & Robbins 1997), and the interpretation of the hydrochemistry must consider possible mixing of groundwater from different horizons. At Moreppen I (Swendesen et al. 1997), water samples

Parameter/ units in mmol/l	Precipitation	Percolation water	Unsaturated zone	Saturated zone / upper	Saturated zone / lower
pH	4.38	3.76	5.88	6.55	7.85
Chloride	0.014	0.028	0.044	0.039	0.079
Nitrate	0.032	0.111	0.011 as N		
Sulfate	0.022	0.044	0.043	0.057	0.149
Sodium	0.012	0.024	0.062	0.079	0.125
Potassium	0.002	0.004	0.027	0.014	0.027
Calcium	0.003	0.006	0.052	0.069	0.662
Magnesium	0.002	0.004	0.019	0.030	0.105
Ammonium	0.024	0.000	0.0014 as N		
Alkalinity			0.06	0.131	1.336
Silicon			0.19	0.131	0.158
PO2	10-0.7	10-0.7	10-0.7	10-0.7	
PCO2	10-3.5	10-3.5/-1.5	10-2.0/-2.8	10-2.4	

Table 1. Chemical development of water at Gardermoen. Average values from: Jørgensen et al. (1991), Skaarstad (1996), Basberg et al. (1998) and Dagestad (in prep.).

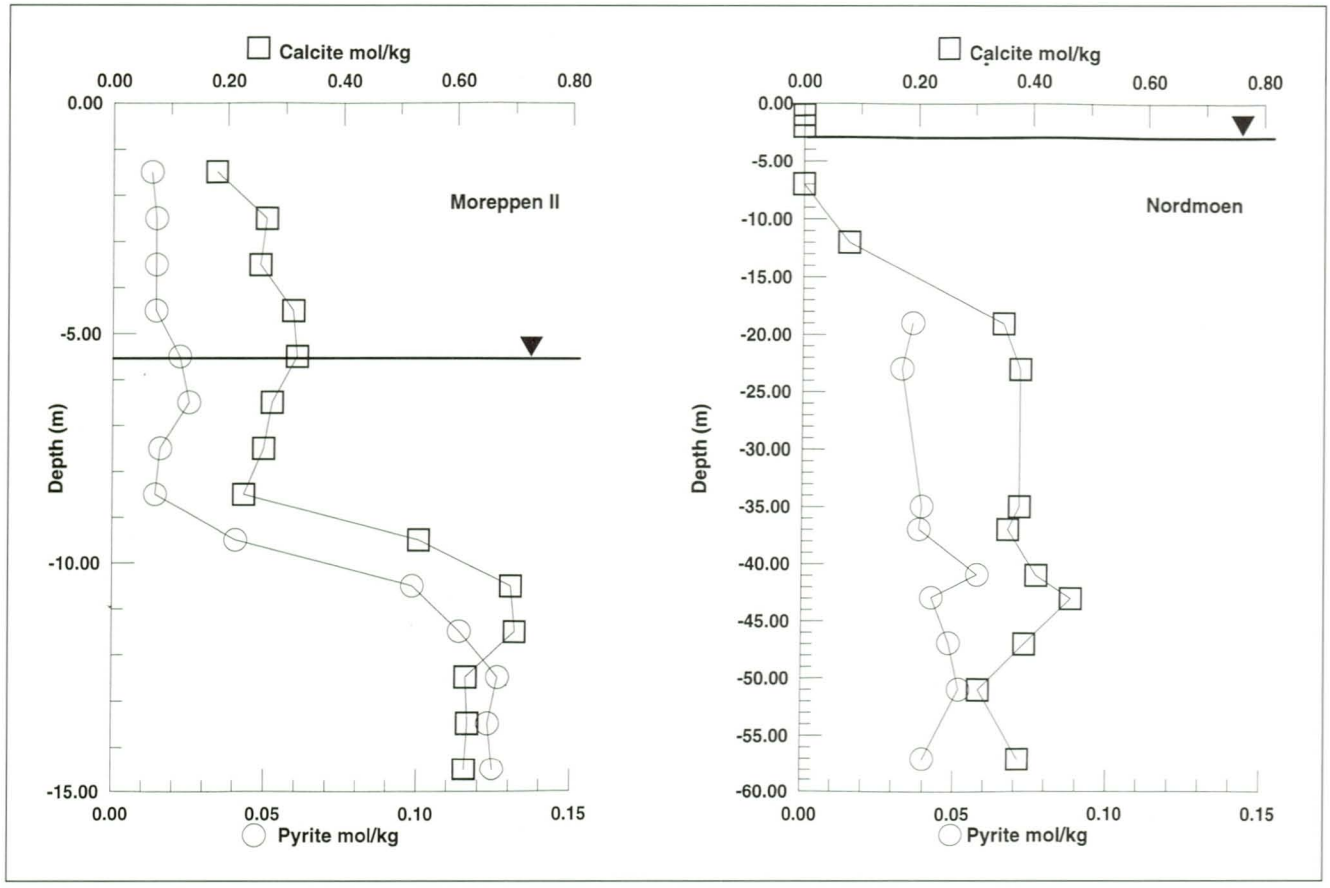

Fig. 3. Observed sediment concentrations, Data for Moreppen II after Dagesstad (in prep.) and data from Nordmoen after Jørgensen et al. 1991.

collected from filters located 2-7 and 6-9 m.b.s. show no traces of pyrite or calcite weathering. Groundwater from a well located at 34-36 m.b.s. has a chemical signature that suggests that these weathering processes have occurred, but unfortunately no samples have been collected between 9 and 34 m.b.s. In connection with the description of a landfill leachate plume at Trandum (Sæther et al. 1992, Basberg et al. 1998), water samples have been collected from wells unaffected by antrophogenic activities. The depths to the pyrite oxidation zone and the calcite dissolution front in these wells are also suggested to be approximately three metres below the groundwater table.

The sediment sampling interval at Nordmoen is too large to confirm if these horizons are located at the same depth at this locality. However, collected data suggest that the calcite weathering horizon is located at approximately 7 m below the water table and that the pyrite horizon is less than 16 m below the water table (Jørgensen et al. 1991).

In general, the vertical resolution is not fine enough to determine, with confidence, the depth to the weathering horizon except in the profile measured by Dagestad (1998) at Moreppen II. However, all sites indicate a horizontal stratification of the aquifer with respect to pyrite and calcite. In the remainder of this report the cited dissolved concentrations from the upper oxic/low ionic strength and lower anoxic/high ionic strength zones are average concentrations taken from available sources using selected wells (Table 1). As for the sediment concentrations, a selection of minerals and values from Jørgensen et al. (1991) and Dagestad (in prep.) has been used.

Model set-up and processes

The sharp boundaries observed between the calcite/decalcified zone and the reduced/oxidized zone suggest that the dissolution of calcite and oxidation of pyrite occur at a rate that is much higher than that of the downward transport of water. Consequently, the assumption of equilibrium seems justified (Rubin 1983). An equilibrium code such as PHREEQC (Parkhurst 1995) can be used to assist in the interpretation of the weathering processes. The program includes a suite of aqueous geochemical reaction models that can be used for the analysis of a wide variety of geochemical problems. Only a few of the options available are used here. These options include; speciation and saturation index, mineral and gas equilibria, and advective-transport modelling. Even if equilibrium not can be assumed, the use of such codes can provide valuable insight into the reaction mechanisms, and can often be a valuable tool for assessing possible weathering scenarios.

A model aquifer has been constructed based on information on the groundwater chemistry and mineralogy of

the Gardermoen aquifer. Forty mixing cells were used representing a 6 m-deep profile. A selection of minerals has been chosen from the unweathered sediment mineralogy, as given in Table 2, and horizons observed at Moreppen II will be used to check the simulation results of the proposed model.

The unsaturated zone has been assumed to be depleted of calcite and pyrite, and this is also indicated by the collected sediment samples. Modelled recharge water introduced into the 'first unweathered cell' is in equilibrium with expected oxygen and carbon dioxide pressures in the lower part of the unsaturated zone (Table 3). The composition of infiltrating water is constant throughout the simulation, and the composition is the same as that found in the decalcified/pyrite-free zone in the upper saturated zone (Table 1). The infiltrating water is transported into the first cell, then water from the first cell into the second, and so forth. The cell shifts are simulating advective transport.

Vertical pore water velocities are calculated from observed average groundwater flow. The vertical component of groundwater velocities varies greatly across the aquifer, but values between 0.6 and 1.2 metres/yr are representative (Jørgensen & Østmo 1990, Basberg et al., 1998). The dimensions of the computational cells are 0.15*0.15*0.15 m, and the effective porosity is 0.3.

Sediment analyses of the calcite and pyrite contents in weathered and unweathered samples from two different locations at the Gardermoen aquifer are shown in Fig 3. The difference in weathered and unweathered calcite concentrations is approximately 0.30 mol/kg with a variation of 0.1 mol/kg. Sediment samples from Moreppen II, Nordmoen and Trandum all reveal similar changes in concentrations, and the adopted initial value of 0.30 mol/kg for the reactive part of the calcite is therefore believed to be representative for the Gardermoen aquifer. Mineral concentrations in each cell are given in moles. Henceforth, the reported values must be multiplied by the bulk density. Reported dry bulk densities vary between 1400-1700 kg/m^3 (Jørgensen et al. 1991, Dagestad in prep.). The calcite concentrations per cell range from 0.9 to 2.2 moles per cell and a concentration of 1.275 moles has been chosen. The reported pyrite concentrations are not as consistent as the calcite concentrations; reported values at Moreppen are approximately a factor of two higher than the concentrations found at Nordmoen. Reported pyrite concentration ranges from 0.03 mol/kg to 0.1 mol/kg, giving a concentration per cell ranging from 0.15 to 0.62 moles. In this study, a value of 0.214 moles has been chosen.

Group	Mineral	Wt.%
Primary		
Amphibole	Hornblende	2.0
	Chlorite	7.0
K-Mica	Biotite	2.0
K-Mica	Muscovite	12.5
	K-Feldspar	17.5
	Plagioclase	8.0
	Quartz	48.0
	Calcite	2.5
	Pyrite	0.5
Secondary		
	Vermiculite	
	Imogolite	
	Oxides	
	Carbonates	
	Oxyhydroxides	

Table 2. Mineralogy at Gardermoen, modified after: Teveldal et al. (1990), Jørgensen et al. (1991) and Dagestad (in prep.)

Pyrite oxidation has been studied intensively by several authors (Nicholson et al. 1988, Postma et al. 1991, Appelo & Postma 1993, Stumm & Morgan 1995, Elberling 1996). The processes included in the model are simplified by assuming that oxidation proceeds at redox equilibrium and equilibrium dissolution. The following reactions (Appelo & Postma 1993) describe the process of pyrite oxidation and precipitation of iron hydroxides.

$$FeS_2 + 7/2O_2 + H_2O = Fe^{2+} + 2SO_4^{2-} + 2H^+ \quad \text{(i)}$$
$$FeS_2 + 14Fe^{3+} + 8H_2O = 15Fe^{2+} + 2SO_4^{2-} + 16H^+ \quad \text{(ib)}$$
$$Fe^{2+} + 1/4O_2 + H^+ = Fe^{3+} + 1/2H_2O \quad \text{(ii)}$$
$$Fe^{3+} + 1/2H_2O = Fe(OH)_3 + 3H^+ \quad \text{(iii)}$$
$$Fe^{3+} + 2H_2O = FeOOH + 3H^+ \quad \text{(iiib)}$$

In the model, goethite (iiib) has been chosen to precipitate rather than ferrihydrite (iii).

The energy yield of (i) is much higher than (ii), so incomplete oxidation may occur and a solution rich in dissolved Fe^{2+} will result if the pH is not increased. The limiting step for pyrite oxidation is believed to be the oxidation of Fe^{2+} (ii). At a pH of around 4, the kinetic control shifts:

1. At pH<4, the reaction is slow and independent of pH.
2. At pH>4, the reaction rate increases rapidly, but is limited by increasing insolubility of iron oxyhydroxides at increasing pH. A secondary mechanism for pyrite oxidation is by Fe^{3+} (ib), but the solubility decreases with a pH increase to the power of 3, so it is only significant at low pH.

Cell	Pyrite moles	Calcite moles	Goethite moles	PCO2	PO2	grw composition
0	-	-	-	10-2.4	10-0.7	upper
1-40	0.2142	1.275	0.002	-	-	deep

Table 3. Initial conditions at 6° Celsius.

The infiltrating water is equilibrated at a given carbon dioxide pressure to give a dissolved carbon dioxide concentration. As the water enters the saturated zone, the system can be characterised as a closed system dissolution of calcite and the amount of calcite that dissolves is determined by the amount of infiltrating carbon dioxide. A simplified reaction on representing calcite dissolution is (Appelo & Postma 1993);

$$CaCO_3 + CO_2 + H_2O = Ca^{2+} + 2HCO_3^- \quad \text{(iv)}$$

If a source of carbon dioxide is present, dissolution of calcite will take place. The solubility of calcite will not solely be controlled by the supply of dissolved carbon dioxide. As pyrite is oxidized, the released protons can associate with the carbonate ion and increase the solubility of calcite. An interpretation of different calcite dissolution mechanisms is given by Plummer et al. (1978):

$$CaCO_3 + H^+ = Ca^{2+} + HCO_3^- \quad \text{at pH<3.5} \quad \text{(v)}$$
$$CaCO_3 + H_2CO_3^* = Ca^{2+} + 2HCO_3^- \quad \text{at 3.5<pH<7.0} \quad \text{(vi)}$$
$$CaCO_3 + H_2O = Ca^{2+} + 2HCO_3^- + OH^- \quad \text{at pH>7.0} \quad \text{(vii)}$$

Calculations to determine the dominating calcite dissolution mechanism indicate that calcite dissolution due to buffering of excess protons from pyrite oxidation and from infiltrating carbon dioxide accounts for approximately one half each of the total dissolution.

The saturation index (SI) for pyrite and calcite is set to -0.6 and -0.5. These levels of undersaturations are primarily used to correct the pH value. Since the model only includes a selection of minerals, the undersaturation may be justified as a means to estimate actual values as would be expected in a system in which the entire mineral matrix was included. Skaarstad (1996) found iron oxyhydroxides in the upper eight metres of the soil profile, and it is postulated that these iron oxyhydroxides are precipitated at the calcite dissolution front after oxidation of pyrite since the pH lowering is buffered due to calcite dissolution. Postma et al. (1991) suggested «that easily extractable iron oxyhydroxidies may accumulate above the redox line, but no obvious relationship exists». In the model application reported by Postma et al. (1991) undersaturation of goethite was used to simulate dissolution of more stable iron oxyhydroxides than goethite, which acted as a pH buffer. In the current model, goethite is included in order to precipitate iron oxyhydroxides. Field data from Moreppen did not reveal high dissolved iron concentrations, suggesting that iron quickly precipitates.

When the physical and chemical characteristics of the sediments and groundwater have been determined, the initial conditions and length of simulation period must be selected. The aim of the model is to reproduce the depth of the weathering horizons since deglaciation, and the simulation period is therefore set to 10,000 years. Since the weathering processes have occurred over such a long time span, many uncertainties are clearly associated with the simulated results.

Results

The development of the weathering horizons is depicted using cell 2 (i.e. 0.15 - 0.30 m below the water table) as the fronts develop from 752 to 833 years (Figs. 4 and 5). This period is selected since it coincides with the major geochemi-

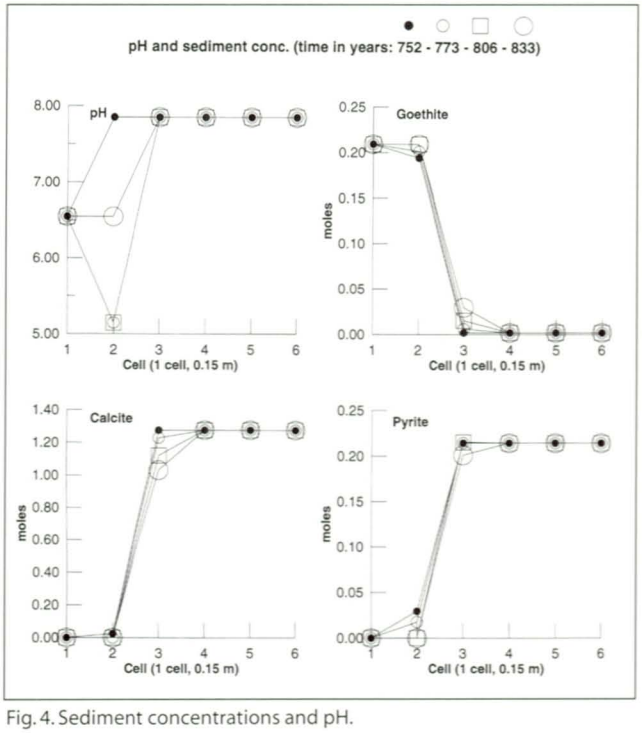

Fig. 4. Sediment concentrations and pH.

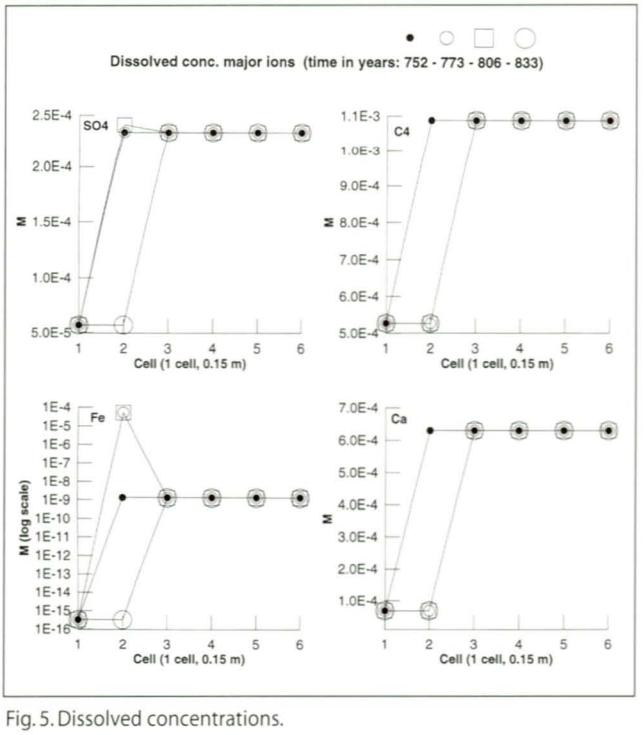

Fig. 5. Dissolved concentrations.

cal developments in the column corresponding to: 1. initial condition, 2. calcite depletion, 3. pyrite depletion, and 4. completely weathered condition. The other cells are depleted in the same sequential fashion down through the column, and a constant rate of increasing calcite depleted/low pH zone over time is quickly approached.

The sediment concentrations and groundwater pH are shown in Fig. 4. A lowering of pH as a result of calcite depletion and ongoing pyrite oxidation is seen in cell 2 until inlet conditions are established. When the cell is depleted of calcite, goethite can act to buffer the acidity, but goethite dissolution is not seen to any significant degree. In cell 2, in which calcite has been depleted, a slight increase in pyrite oxidation due to the increased dissolved Fe^{3+} concentrations is seen from the calculations. Since calcite dissolution is partly controlled by pyrite oxidation, it was expected that the increased pyrite oxidation would affect the calcite dissolution in the next cell, but a significant increase has not been observed.

From these simulations with a flow velocity of 0.9 m/yr it would take 9000 years to weather a 3.2 m-thick profile. Henceforth, the simulated results suggest that the selected average vertical velocity of 0.9 m/yr is slightly higher than the actual vertical velocity in the area. The solubility of dissolved iron is strongly dependent upon pH. Dissolved Fe^{2+} concentrations will be stoichiometrically controlled by incomplete pyrite oxidation at low pH. At low pH, the energy differences between the oxidation of iron and sulphide will be determining for the dissolved iron concentration, but as pH increases, iron will precipitate due to insolubility of iron oxyhydroxides resulting in small dissolved concentrations.

Dissolved concentrations of selected species between 752 and 833 years are shown in Fig. 5. The concentrations show an increased amount of dissolved iron, and the shift coincides with the depletion of calcite in the cell and the associated lowering of pH to approximately 5. An increased pyrite oxidation due to lack of calcite buffering is noted in the calculations, and a slight increase in aqueous sulphate can be seen. The aqueous Fe^{2+} concentrations are closer to the calculated values using incomplete pyrite oxidation due to infiltrating dissolved oxygen (equation: i) in the low-pH zone. As the solution is transported into the calcite dissolution zone, equilibrium is shifted as the pH increases, and the result is a complete pyrite oxidation.

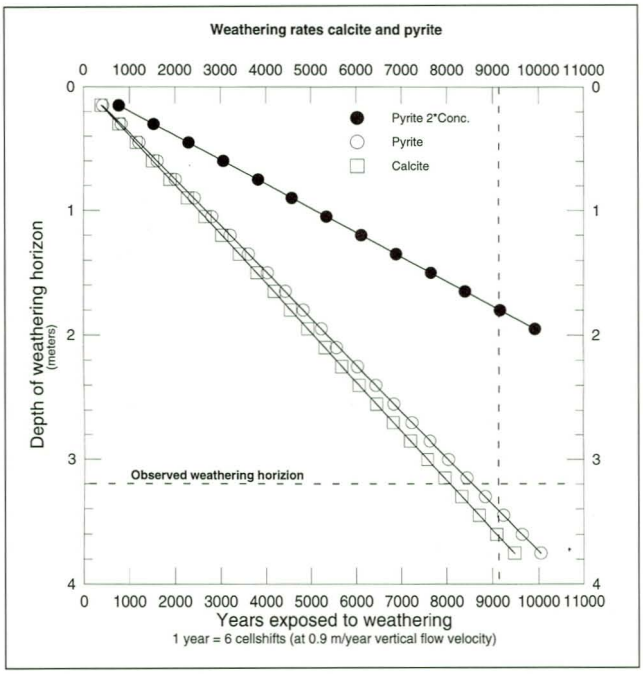

Fig. 6. Rates of calcite and pyrite depletion.

Variation in saturation indices influences the simulated pH value in the different horizons. This influence is most critical for calcite (Table 4). For pyrite and goethite, the range of saturation indices used does not influence the pH to the same extent, and the variations only result in a minor change in pH. The simulated pH values for the base case agree well with the observed pH in the completely weathered and in the unweathered zones. Unfortunately, no measurements have been made in the intermediate zone.

The rates of calcite and pyrite depletion are shown i Fig. 6. Both rates are almost linear, but it was expected that the lowering of pH in the decalcified zone might have increased the weathering rates over time. This influence on the overall rates can't be detected in these simulations. The regression equations describing the propagation of the pyrite oxidation and calcite dissolution fronts are given by:

Calcite dissolution :Y = 3.96*10-4*X - 3.43 *10-3
Pyrite oxidation :Y = 3.74*10-4*X - 3.57 *10-3

			pyrite & calcite free zone	calcite free zone	unweathered
Observed SI Pyrite	SI Calcite	SI Goethite	6.55	n.a.-	7.85
-0.6	-0.5	-1.5	6.55	5.14	7.85
0.0	0.0	0.0	6.55	5.82	8.40
0.0	0.0	-1.5	6.55	5.16	8.40
0.0	-0.5	-1.5	6.55	5.16	7.85
-0.6	0.0	-1.5	6.55	5.14	8.40

Table 4. Observed (average) and simulated pH at different SI.

where Y is the thickness of weathering horizon (metres), and X is the time exposed to weathering (years).

The influence of different sediment concentrations is also depicted in Fig. 6, where a doubling of the pyrite content leads to a decrease in the movement of the pyrite oxidation front, as expected. The rate of propagation is one half of the original propagation rate, and generally we can say that the rate of propagation is linear.

Jørgensen et al. (1991) suggested that three metres of the aquifer should be free of pyrite, while a 10 m-thick horizon should be decalcified based on mass balance studies. The PHREEQC simulations yield results that are in good agreement with the depth of the pyrite-free zone. Unfortunately, the good agreement is partly due to a coincidence. Jørgensen et al. (1991) used an oxygen consumption of 0.25 mmol/l while the current study suggests that the oxygen consumption should be higher, approximately 0.32 mmol/l; henceforth the current study should predict a deeper pyrite-free zone, but the pyrite concentrations used in the two studies are such that the oxidation front is located at the same depth (since different dry bulk densities have been used). Jørgensen et al. (1991) suggested from mass balance studies that approximately 50% of the bicarbonate in the aquifer results from calcite dissolution and carbon dioxide. The same distribution was found in this study, but the thickness of the decalcified zones does not agree in the two studies. The deviations can't be explained by different dry bulk densities. A more likely source of the error is that of problems with an unknown source of calcium. Teveldal et al. (1990) concluded that there must be another source for calcium. The same problem may have caused an overestimation of the thickness of the weathering horizons, as suggested by Jørgensen et al. (1991).

The pyrite concentration of 0.03 mol/kg is approximately ten times the concentration reported by Postma et al. (1991), and the propagation of the pyrite-free horizon is approximately ten times slower at Gardermoen, and a much shallower pyrite-free horizon is found. The thinner oxic- saturated zone makes the aquifer more vulnerable to possible contamination.

The observed horizons versus predicted horizons are shown in Fig. 7. The vertical velocity has been corrected to 0.8 m/yr in order to obtain an almost exact fit. The vertical velocities are one of the key parameters in the model. With the reported velocities ranging from 0.6 to 1.2 m/yr for the Gardermoen aquifer, a reasonable fit can be obtained.

Discussion and conclusion

Items that will be important for the modelling results are; variation in the mineralogy, partial gas pressure at the water table, aqueous species in infiltrating water, groundwater velocities, flow pattern, location of the groundwater table in a geological time perspective, and variation in precipitation,

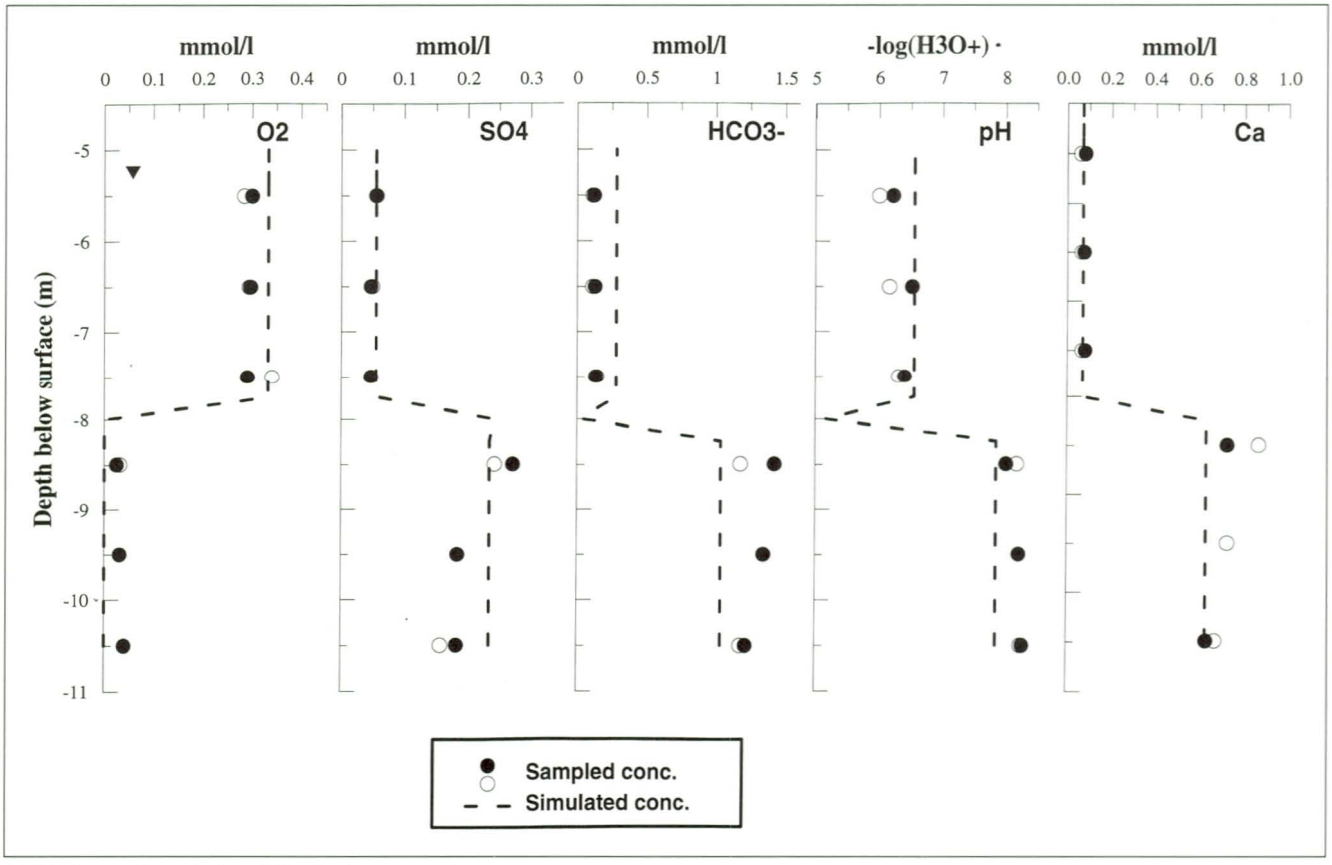

Fig. 7. Observed vs. calculated dissolved concentrations.

both seasonal fluctuations and fluctuations on a geological time scale. Areas in which the reported model can be improved by further field work are in the determination of mineralogy and dissolved gas concentrations. The reported values show some variation, and it would be beneficial to obtain more conclusive field data from the Gardermoen reservoir.

In the model, pyrite and calcite weathering in the unsaturated zone has been neglected since these processes have occurred so fast that they can be assumed to be instantaneous on a geological time scale. It is suggested that increased oxidation and dissolution occurred just after the deglaciation with a rapid lowering of the water table and exposure of the freshly grained surfaces to the atmosphere. This may have produced a hydrochemical environment that is different from the one seen today, due to more extreme conditions. The determination of the maximum depth to the water table on a geological time scale is crucial to obtaining reasonable results from the model since the point of zero propagation is assumed at the water table. With the available information on groundwater fluctuations and controls on water table location, the measured water table from 1996 seems to be a reasonable divide between an unsaturated and saturated zone.

Sediment concentrations are another factor that will control the simulated results (Postma et al. 1991), as depicted in Fig. 6, where a doubling of the pyrite concentration is shown together with selected concentrations. The increased pyrite concentration did not affect the downward movement of the calcite dissolution front. If the relative concentrations of calcite and pyrite in the sediments are such that the two fronts are not located at approximately the same depth, it would be expected that some other buffering mechanism than calcite would be active in the decalcified zone, or that a low-pH zone should be found in the aquifer. From samples collected across the aquifer no low-pH zone is found, and the hydrochemical signature is fairly uniform with either calcite and pyrite weathering products or low ionic strength water, suggesting that no significant pyrite oxidation or calcite dissolution have occurred. The field observations support the simulated results that the pyrite and calcite transition zones are located at approximately the same depth. The results also suggested that the calcite front is located slightly below the pyrite front. If the calcite front was located above or at the same depth as the pyrite front, the alkaline environment would negate pyrite oxidation (Nicholson et al. 1988) and the pyrite-depleted zone could not have been reproduced using the reported approach. There are some uncertainties associated with the selected pyrite concentration due to an inconsistency in reported concentrations. However, when evaluated together with the calcite content, for which the analytical results are more consistent, the selected concentration for pyrite seems reasonable. This does not exclude the possibility that there may be areal variations in sediment concentrations and that the depth to the depleted zones may vary across the aquifer, but it is suggested here that the relative concentration of pyrite to calcite will be fairly uniform across the aquifer. This might be explained by the mineralogical analyses that suggest that both minerals reside in the shale fraction of the sediments. It would be instructive to obtain more field data in order to disclose any areal variation, determine the concentration with a higher level of accuracy, and disclose possible variations between the different depositional structures.

Silicate weathering is not accounted for in the model, and henceforth its contribution to the aqueous chemistry is not evaluated quantitatively. The exclusion of these minerals may also lead to an overestimation of calcite weathering, since possible buffering of pH by silicates is neglected. The hydrochemistry indicates that the contribution to water chemistry across the weathering horizon is primarily derived from pyrite oxidation or calcite dissolution. Increase in species indicating silicate weathering are orders of magnitude smaller. In addition to silicate weathering, an observed increase in manganese across the weathering horizon may be explained by additional buffering by manganese oxides. It is expected that the additional buffering will be most active in the decalcified zone just below the pyrite oxidation zone. In the reduced leachate plume originating from the Trandum landfill a reduction of sediment- bound iron and manganese has been observed, suggesting that there are considerable iron and manganese oxides and oxyhydroxides available in the aquifer sediments (Basberg et al., 1998). For minerals for which equilibrium can't be assumed a kinetic approach must be employed. Nystrøm et al. (1995) have reported a model in which chemical kinetics of aluminum silicate minerals are included. Their model has been constructed based on the PHREEQE model, and a similar approach could be employed in a future study, where a selection of the most active minerals could be tested against observed weathering in the field.

When the focus is shifted to the movement of anthropogenic contaminants, natural weathering processes will contribute significantly less than anthropogenically induced changes. However, an understanding of the natural geochemical environment in the aquifer forms the basis for an evaluation of the movement of anthropogenic contaminants. The distinct separation and thickness observed of the oxic and anoxic zone will influence leachate migration, depending upon which zone the leachate resides in. The velocities and flow pattern in the area, especially in the vicinity of the Trandum landfill, are complex due to highly heterogeneous nature of the sediments in this area (Basberg et al. 1998). To assess the importance of the flow pattern it is necessary to couple flow and solute transport with the geochemical reactions. These results will provide a better understanding of how the depth of the pyrite and calcite horizons varies with the hydrogeological flow pattern.

Interpretation of the current simulations requires that the user is aware of the constraints that are imposed on the model. Nevertheless, the simulations do mimic the field ob-

servations, and the main features of propagation of the calcite- and pyrite-depleted horizons seem to be captured by the model. Observed weathering horizons at 3 m below the water table of pyrite and calcite have been reproduced using the PHREEQC geochemical model on a geological time scale. The model also predicted a low pH and decalcified zone located between the completely weathered and unweathered zone of the aquifer. This zone was expected, but no evidence has been collected since the microscreens were placed vertically too far apart. The determination of the dominating natural geo-/hydrochemical environment will be the starting point for future investigations of landfill leachate migration in the aquifer at the Trandum landfill, including simulations of coupled flow, solute transport and geochemistry.

Acknowledgments

We thank the Research Council of Norway for funding. Critical reading of the manuscript by Ola Magne Sæther and Steven A. Banwarth are greatly appreciated, as their suggestions have greatly improved this paper. Special thanks are extended to Kirsten Djørup and David Roberts for their linguistic comments on the manuscript.

References

Andersen, B.G. & Borns, H.W. Jr. 1994: *The Ice Age World*, Scandinavian University Press, 208 pp.

Appelo, C.A.J. & Postma, D. 1993: *Geochemistry, groundwater and pollution*, A.A. Balkema Publishers, 536 pp.

Basberg, L., Banks, D. & Saether, O.M. 1998: Redox processes in groundwater impacted by landfill leachate. *Aquatic Geochemistry* (in press).

Elberling, B. 1996: *Oxygen gas transport and consumption in the unsaturated zone*. Ph.D. Thesis, Department of Earth Sciences, University of Aarhus, Denmark, 184 pp.

Gustafsson, J.P., Bhattacharaya, P., Bain, D.C., Fraser, A.R. & McHardy, W.J. 1995: Podzolization mechanisms and the synthesis of imogolite in Northern Scandinavia. *Geoderma 66*, 167 - 184.

Jørgensen, P. & Østmo, S.R. 1990: Hydrogeology in the Romerike area, Southern Norway. *Norges geologiske undersøkelse Bulletin 418*, 19 - 26.

Jørgensen, P., Stuanes, A.O. & Østmo, S.R. 1991: Aqueous geochemistry of the Romerike area, Southern Norway. *Norges geologiske undersøkelse Bulletin 420*, 57 - 67.

Kirkhusmo, L.A. & Sønsterud, R. 1988: Overvåking av grunnvann, landsomfattende grunnvannsnett (in Norwegian). *Norges geologiske undersøkelse Rapport 88.046*, 72 pp.

Longva, O. 1987: Ullensaker 1915 II Beskrivelse til kvartærgeologisk kart M 1:50000. *Norges geologiske undersøkelse Skrifter 76*, 39 pp.

Martin-Hayden, J.M. & Robbins, G.A. 1997: Plume distortion and apparent attenuation due to concentration averaging in monitoring wells. *Ground Water 35*, 339-346.

Nicholson, R.V., Gillham, R.W. & Reardon, E.J. 1988: Pyrite oxidation in carbonate-buffered solution: 1. Experimental kinetics. *Geochimica et Cosmochimica Acta 50*, 1077-1085.

Nystrøm Claesson, A. & Anderson, K. 1996: PHRQKIN, A program simulation dissolution and precipitation kinetics in groundwater solutions. *Computers & Geoscience 22*, 559 - 657.

Parkhurst, D.L. 1995: User's guide to phreeqc- a computer program for speciation, reaction-path, advective-transport, and inverse geochemical calculations. *U.S. Geological Survey, water-resources investigations report 95-4227*, 143 pp.

Plummer, L.N., Wigley, T.M.L. & Parkhurst, D.L. 1978: The kinetics of calcite dissolution in CO_2 water systems at 5° to 60° Celsius and 0.0. to 1.0 atm CO_2, *American Journal of Science 278*, 179-216.

Postma, D & Brockenhuss-Schack, S.B. 1987: Diagenesis of iron in postglacial sand deposits of late- and post-Weichselian age. *Journal of Sedimentary Petrology 57*, 1040-1053.

Postma, D., Boesen, C., Kristiansen, H. & Larsen, F. 1991: Nitrate reduction in an unconfined sandy aquifer: water chemistry, reduction processes, and geochemical modeling. *Water Resources Research 27*, 2027-2045.

Reardon, E.J., Allison, G.B. & Fritz, P. 1979: Seasonal chemical and isotopic variations of soil CO2 at Trout creek, Ontario. *Journal of Hydrology 43*, 355-371.

Rubin, J. 1983: Transport of reacting solutes in porous media: relation between mathematical nature of problem formulation and chemical nature of reactions. *Water Resources Research 19*, 1231-1252.

Rudolph-Lund, K. 1997: *A three-dimensional gradient tracer study in the Romerike aquifer near the Gardermoen international airport*. Cand. Scient. Thesis, Department of Geology, University of Oslo, April 1997, 108 pp.

Skaarstad, B. 1996: *Undersøkelse av løsmassene ved Moreppen, Gardermoen. Fysisk sammensetning, mineralogi og vannkjemi.* Hovedoppgave ved institutt for jord- og vannfag, Norges Landbrukshøgskole. Rapportserie C, 40 pp (In Norwegian).

Stumm, W. & Morgan, J.J. 1996: *Aquatic chemistry - chemical equilibria and rates in natural waters 3 rd* ed., John Wiley & Sons, New York, 1022 pp.

Sæther, O.M., Misund, A., Ødegård, M,. Andreasen, B.Th. & Voss, A. 1992: Groundwater contamination at Trandum landfill, Southeastern Norway. *Norges geologiske undersøkelse Bulletin 422*, 83-95.

Swensen, B. & Singh, B.R. 1997: Transport and transformation of urea and its derivatives through a mineral subsoil. *Journal Environmental Quality 26*, 1516-1523.

Teveldal, S., Jørgensen, P. & Stuanes, A.O. 1990: Long-term weathering of silicates in a sandy soil at Nordmoen, Southern Norway. *Clay Minerals 25*, 447-465.

Tuttle, K.J. & Aagaard, P. 1996: *Depositional processes and sedimentary architecture of coarse -grained ice contact Gardermoen delta, Southeast Norway*. In Aagaard P & Tuttle K.J. (eds) Proceedings to The Jens-Olaf Englund Seminar - Protection of groundwater resources against contaminants. Department of Geology, University of Oslo, 181-223.

Østmo, S.R. 1976: Hydrogeologisk kart over Øvre Romerike. Scale 1:20000. *Norges geologiske undersøkelse.*

Manuscript received January 1998: revised manuscript accepted June 1998.